

Article

Time-resolved characterization of dynamic tribochemical processes for dicationic imidazolium ionic liquid

Roman Nevshupa ^{1,*}, Marcello Conte ², Silvia Guerra ³ and Elisa Roman ³

¹ Spanish National Research Council, Institute "Eduardo Torroja" (IETCC-CSIC), C/Serrano Galvache 4, 28033 Madrid, Spain; r.nevshupa@csic.es

² Anton Paar TriTec SA, Rue de la Gare 4, 2034 Peseux, Switzerland; marcello.conte@anton-paar.com

³ Spanish National Research Council, Institute of Material Science of Madrid (ICMM-CSIC), C/Sor Juana Inés de la Cruz 3, 28049 Madrid, Spain; silvia.guerra@csic.es

* Correspondence: r.nevshupa@csic.es; Tel.: +34-913-020-440

Abstract: Dynamic tribochemical processes for dicationic ionic liquid containing a germinal imidazolium cation head groups bridged by a poly(ethylene glycol) and bis(trifluoromethylsulfonyl)imide anion were studied using time-resolved Mechanically Stimulated Gas Emission Mass-Spectrometry (MSG-MS). In comparison with similar monocationic imidazolium ionic liquids with short alkylic or long polyether side chains the dicationic ionic liquid had lower coefficient of friction on Ti6Al4V alloy and smoother behaviour. The analysis of volatile decomposition products suggested multiple tribochemical reactions in which both anionic and cationic moieties are involved. Tribochemical degradation of cations was mainly through detachment of the side and bridging chains from the imidazolium head groups. Absence of volatile products containing nitrogen implies that imidazole group remained unchanged. Hydrogen and water desorption were attributed to the reactions of hydrogen fluoride being a product of anion degradation with titanium and titanium oxide.

Keywords: Ionic liquids; dicationic; imidazolium; poly(ethylene glycol); tribochemistry; mechanically stimulated gas emission mass-spectrometry

1. Introduction

Room-temperature Ionic Liquids (ILs) are salt structures consisting of large cation and anion moieties, which are characterized by melting temperatures below 100 °C. In tribological applications, the ILs have demonstrated superior performance as lubricants under both mixed and boundary conditions [1-9]. Under severe environments, in space and at high temperatures IL-base lubricants are especially propitious due to their exceptional tribochemical thermal and stability, both oxidative and nonoxidative [10-14]. During the last decade imidazolium-base ionic liquids with fluorinated anions have been specially addressed in a number of studies [1,15-17]. The application range of the imidazolium ILs was further expanded by rational designing of the molecular structure and side chains offering the possibility of obtaining versatile ILs with tailored polarity, hydrophobicity, corrosive and antioxidant properties [7,18-25]. Generally, the increase of the length of alkyl side chains attached to a cation head group leads to improvement of wear resistance, but this effect is not straightforward [2,22,26]. Substitution of alkyl chains by poly(ethylene glycol) (PEG) improved tribological performance of the IL, although at the cost of decreasing its thermal stability [8,27]. Another approach relies on bridging two cationic head groups by PEG chain. Molecular dynamics simulation and advanced spectroscopy have revealed significant difference in structural

heterogeneity and nano-organization between monocationic and geminal dicationic ILs with long connecting chain [28-31] that is associated with better tribological properties, higher stability, lower toxicity and corrosiveness of the dicationic ILs [14,31-41].

In literature there is a consensus of opinions that the good friction-reduction and wear-resistance properties of ILs owe to their ability to form stable adsorbed layers and protective tribo-films [4,27,42-44]. For ILs with fluorinated anions, Jimenez et al. [26] noted that formation of a metal fluoride-rich boundary tribolayer is necessary to achieve a good tribological performance. Cai et al. [8] studied the changes in the chemical composition of steel surface subjected to rubbing under PEG lubrication with various imidazolium ILs additives and provided the evidences for complicated tribochemical reactions leading to formation of iron oxides, fluorides and sulphates. Physical adsorption of nitrogen double-bond compounds on steel surface was also reported [45]. Mahrova et al. [46] showed that the tribofilms formed by some pyridinium-based dicationic ILs with PEG bridging chain were able to significantly reduce friction in comparison with glycerol base stock, but had much higher wear rate. However, in most of the studies the steps of tribochemical processes laying behind remain poorly understood. In a large measure, this is due to the low yield and selectivity of tribochemical reactions [11] and lacking of a broadly available experimental technique for time-resolved characterization of tribochemical reactions at a buried interface. In the vast majority of experimental studies a *post mortem* approach has been employed that consists in analysing possible chemical changes on the worn surfaces, wear debris and in the lubricants following a tribological test [7,11,47].

A new family of experimental techniques that combine tribometry with mass-spectrometry or surface sensitive techniques has recently emerged [48-54]. These new techniques can provide important information on development of tribochemical processes in the course of a tribological test. In the present work we probed tribochemical processes in dicationic imidazolium ionic liquid with PEG₅₀₀ bridging chain and bis(trifluoromethylsulfonyl)imide (NTf₂) anion on Ti6Al4V substrate using Mechanically Stimulated Gas Emission (MSGE) mass-spectrometry. This material was selected for the substrate because of the technological implications [26] and to be able to contrast the results of this study with previous works [26,44,46]. The tribochemical reactions were analyzed through measuring of the composition and emission kinetics of volatile products as function of the normal load and tests duration. The products of tribochemical reactions were identified using statistical and correlation analyses. The results were compared with the tribochemical behaviour of an homologous monocationic ionic liquid [27,44].

2. Experimental

2.1. Materials

Dicationic geminal imidazolium IL with a polyethyleneglycol (PEG₅₀₀) bridging chain and bis(trifluoromethanesulfonyl)imide anion was synthesized and kindly provided by Dr. M. Mahrova. [46,55]. The structures of the dicationic IL (IL2-di) and its monocationic analogue (IL2) used as a benchmark in this study are shown in Figure 1.

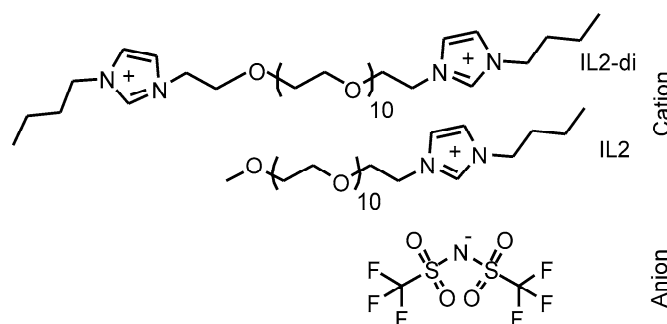


Figure 1. Molecular structures of the dicationic IL and analogue monocationic IL.

A drop of 1 μl of IL was supported on a titanium grade 5 flat sheet. The pin was an alumina ball, 3 mm in diameter. Before each experiment both the substrate and the pin were ultrasonically degreased in acetone and ethanol bath. To eliminate the adsorbed water and air-borne carbonaceous contamination the pin was etched in a hot Piranha solution (3 parts of concentrated sulphuric acid and 1 part of 30% hydrogen peroxide solution) for several minutes.

2.2. Experimental techniques and procedures

Tribological characterization and analysis of mechanically stimulated gas emission were carried out using an original ultrahigh vacuum system [49,50]. A friction cell with a reciprocating pin-on-flat configuration was specially designed to obtain nearly zero intrinsic gas emission. For the sake of comparison with the reference IL, friction force was measured under the same conditions as in the work [44]: the normal load was 9.8 N and mean linear velocity was 2.7 mm/s. The composition of the emitted gases was analysed by a quadrupole mass-spectrometer. During MSGE measurements, the force gauges were off to avoid cross talk, while the experimental conditions were changed to optimize the operating conditions for the mass-spectrometer (avoid amplifier overloading, reduce contamination of the electron multiplier by volatile organic compounds and enhance dynamic response): the normal load was 0.9-1.8 N and the mean sliding velocity was 0.18 m/s. A diaphragm of well-defined molecular conductance situating between a vacuum chamber and a pumping line provided for quantification of the rate of gas emission using a dynamic gas expansion method [56].

High stability of the residual gas pressure is crucial for accurate measuring of tiny pressure variation associated with MSGE. Therefore, the system was kept under pumping until the variation of the mass-spectrometer signals was below 3%/hour, usually for 48-72 hours. With the residual pressure stabilized, the reference mass-spectrum of residual gases was obtained. For this purpose, five or more mass-spectra were measured. These data was organized in a matrix with N columns representing the spectral components with different mass-to charge ratios, m/z , and n_r rows representing the samples of the mass-spectra. The sample mean and the sample standard error were determined column-wise yielding the vectors of size N of a reference mean mass-spectrum, **RMS**, and a reference standard errors, **RSE**, correspondingly.

Mechanically stimulated gas emission was studied by measuring the mass-spectra in the course of rubbing and for several hundreds of seconds after its end. The return of all mass-spectrometry signals to their initial background level was chosen as a criterion for measurement ending. The matrix of the measured data, **MS**, had n rows corresponding to MSGE mass-spectra of N channels each. Differential mass-spectra, **DMS**, characterizing the emitted gases were obtained by subtracting the reference spectrum **RMS** from each row of the matrix **MS**:

$$\|dms_{i,j} = ms_{i,j} - rms_j\|_{i=1,\bar{n};j=1,\bar{N}}; \quad (1)$$

A t -test ($H_0: dms_{i,j}=0$ and $H_1: dms_{i,j}\neq 0$) was used to check the statistical significance of the values of **DMS** [27]. A statistics $\frac{dms_{i,j}}{rse_i}$ was compared with the critical value of Student's distribution, $t_{k,\alpha}$, where $k=n_r$ is the number of degrees of freedom and α is the significance level. The null hypothesis was accepted if

$$\frac{dms_{i,j}}{rse_i} \leq t_{k,\alpha} \quad (2)$$

When a highly dynamic emission process is measured by a mass-spectrometer, the sequential form of channel's measuring may lead to significant increase of the data variation. This may hamper identification of the volatile components being the ion precursors. To face this problem a behavioural analysis of the mass-spectroscopic signals was developed [44,57] and applied in this work. The method is based on the hypothesis that the signals having the same behaviour of the time series should originate from the same precursors. For this purpose the **DMS** was resized by removing null columns, i.e. the null components of the differential mass-spectra, and then Pearson correlation coefficient, r , was calculated for each pair of the DMS components. Statistical significance

of the r was analysed using hypothesis tests with $H_0: r=0$ and $H_1: r \neq 0$. The null hypothesis was rejected if the corresponding p -value was below α .

3. Results and discussion

The behaviour of friction coefficient of IL2-di is shown in Figure 2 (a). Friction coefficient rapidly stabilized without pronounced run-in. The steady coefficient of friction (COF) was about 0.2 - slightly lower, than for homologous monocationic IL2 (see Figure 2 (b)). For comparison, the results of previous study [58] for homologous monocationic IL2 and IL1 (1-butyl-3-methylimidazolium bis(trifluoromethanesulfonyl)imide) are also shown in Figure 2 (b). For dicationic IL with PEG bridging chain the COF decreased on 30% with respect to monocationic IL with alkyl side chains and 10% with respect to monocationic IL with methoxyPEG side chain. These results are in line with literature [14,36,46].

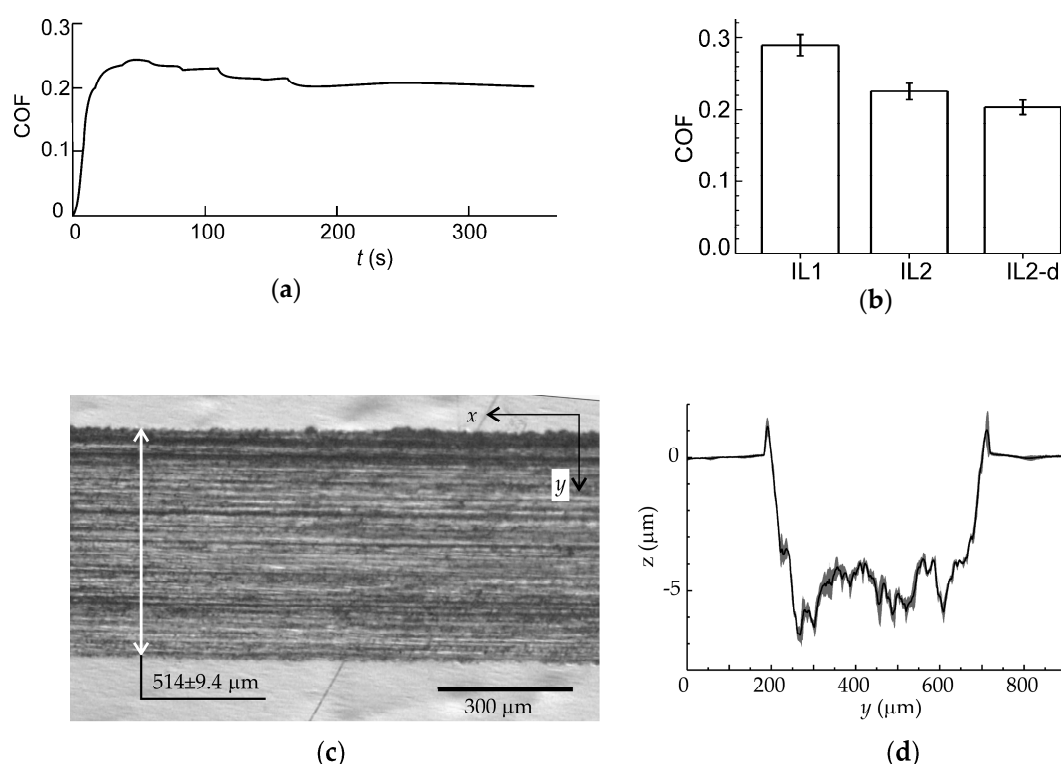


Figure 2. (a) Time series of friction coefficient for dicationic IL2-di. (b) Mean coefficient of friction (COF) and standard error of mean for IL2-di. The data for two homologous monocationic IL2 and IL1 (1-butyl-3-methylimidazolium bis(trifluoromethanesulfonyl)imide) from [44] is also shown for the comparison. (c) Optical image of the worn surface after tribological test. (d) Mean cross-section profile of the wear track. The shaded area depicts the confidence interval ($\alpha=0.05$)

The worn surface (Figure 2 (c)) showed longitudinal abrasion marks. The mean cross-section profile is shown in Figure 2 (d) by a solid line, while the shaded area depicts the confidence interval. The surface morphology was irregular across the wear track (large variation of the height along y), but quite regular in the longitudinal direction (x) that follows from relatively small spread of the confidence interval. Blackish pileups on the sides of the wear track should be related with the products of tribochemical reactions rather than with plastic deformation of the substrate. Presence of blackish deposits on the valleys between the longitudinal marks also points on the possible tribofilm. Wear of the tribofilm together with the substrate corrosion/tribocorrosion could be the reason of changing the colour and transparency of the IL2-di which turned black and opaque after the test. Despite absence of evident corrosion signs immediately after the friction test, corrosion pits appeared on the whole sample surfaces, both rubbed and not, when the samples were kept covered

by IL2-di for several days after the test. The possible mechanisms of corrosion will be discussed at the end of this section.

The differential mass-spectra of volatile products emitted from IL2-di during rubbing (see Figure 3) presented similitude with the DMS of IL2, which were reported previously [44]. For both IL2 and IL2-di the spectral components can be classified into the four groups shown in Table 1.

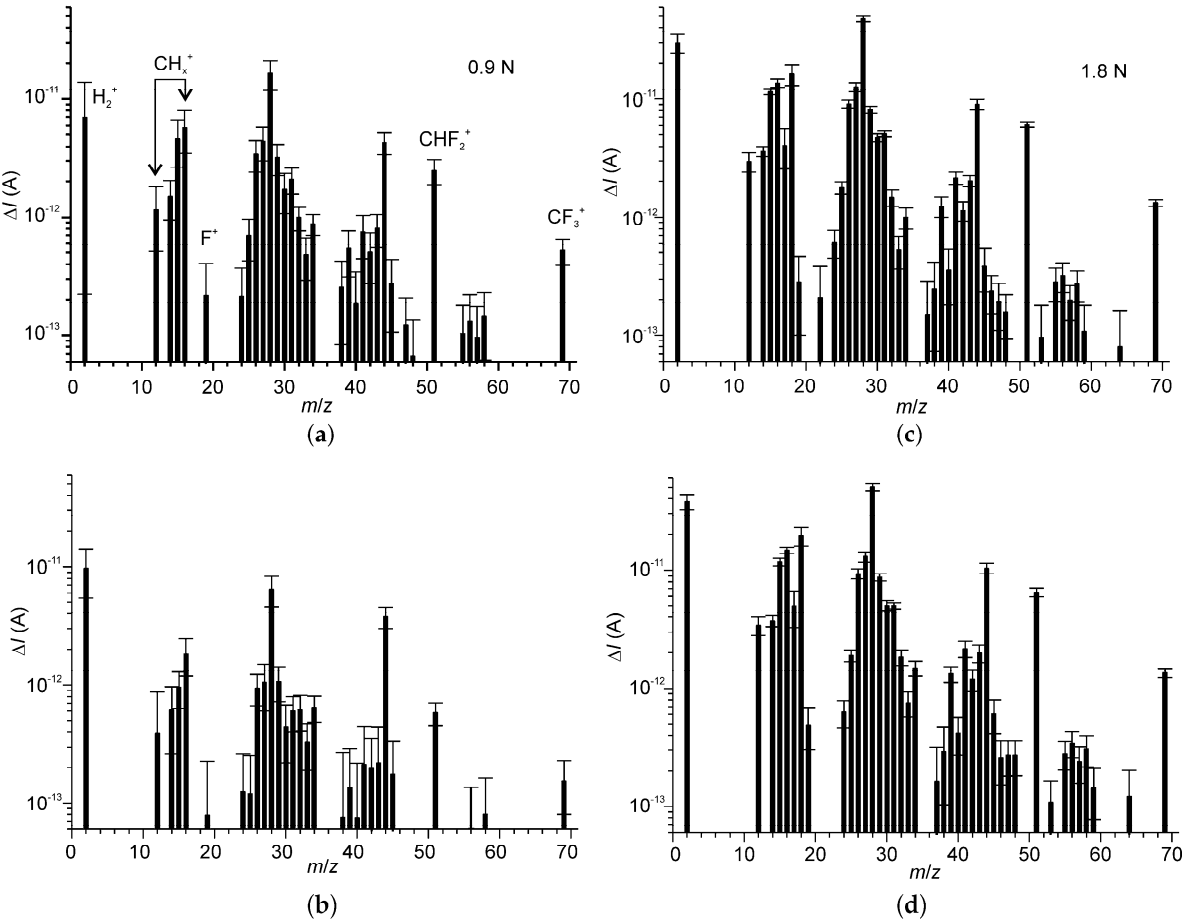


Figure 3. Mean differential mass-spectra (DMS) of emitted volatile products of tribochemical reactions with IL2-di as function of normal load: (a), (b) 0.9 N; (c), (d) 1.8 N. All DMS were obtained during rubbing: (a) and (c) correspond to the initial stage of the test; (b) and (d) correspond to the final stage of the test.

Table 1. Groups of the components of DMS of IL2-di

Group	m/z	Possible precursors
A	19, 31, 32, 51, 69	CF_3 , CF_xH_y , $CF_xH_y^+$, $CF_xH_y^+$, PEG (31, 32)
B	12-16	CH_4 , CH_3^+ , CH_3^+
C	24-34, 39-45, 55-58	PEG, alkanes
D	2, 17, 18	H_2 , H_2O

The group of ions A can be ascribed to volatile compounds originating from the trifluoromethyl detachment from the anion, while the ions at m/z 31 and 32 could also have contributions from PEG fragments. The component at m/z 51 was the most intensive in this group. The signal m/z 50 was excluded from the DMS after the significance test since the null hypothesis was not rejected. This finding contrasts the results obtained for monocationic IL2, for which both m/z 50 and 51 were statistically significant [44]. It also suggests that after detachment from the anion, trifluoromethane recombines with H and reaches the mass-spectrometer as fluoroform rather than carbon tetrafluoride or trifluoromethyl radical. This is supported by the observation that the relative

intensities of the signals at m/z 50, 51 and 69 are in reasonable compliance with the corresponding components of the fragmentation patterns CHF_3 [59] (Figure 4). The large difference between the experimental data and the reference spectra for the signals at m/z 31, 32 can be ascribed to the contributions from CH_3O^+ and CH_4O^+ , respectively. Notwithstanding this difference, the experimental data is closer to the fragmentation pattern of fluoroform, than CF_4 . The signal of F^+ at m/z 19 was weak in all cases, and the differences between the experimental spectrum and the fragmentation patterns were within the measurement uncertainty.

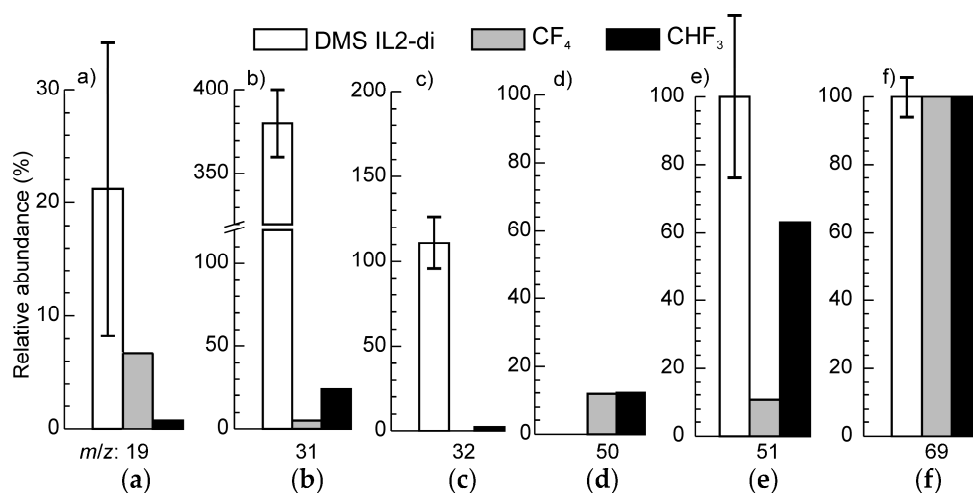


Figure 4. Relative intensities of signals from the group A and fragmentation patterns for electron impact ionization for CF_4 and CHF_3 adapted from [59]. All the data were normalized by the signal m/z 69.

Good correlation was also found between the relative intensities of the signals of group B and the fragmentation pattern for methane (Figure 5). The correct proportion between the ions at m/z 15 and 16 indicates that these ions come from methane rather than from higher alkanes, for which the signal at m/z 16 is lacking. Methane can be formed from methyl radicals in a two-step reaction: i) detachment from the butyl side chains of the cations, and ii) recombination with hydrogen atom extracted from the environment, e.g. from acidic C(2) position on the imidazolium ring [60,61]. This process is promoted by poor proton abstracting ability of the NTf_2^- anion [62]. Previously this model was put forward to explain tribochemical emission of methane from *N*-alkylimidazolium bis(trifluoromethanesulfonyl)imide ILs and IL2 [27,44,48]. Ethyl group of PEG could be another precursor of methane. The radicals have to undergo complete recombination before they reach the mass-spectrometer as it is evidenced from the ratio between m/z 15 and 16.

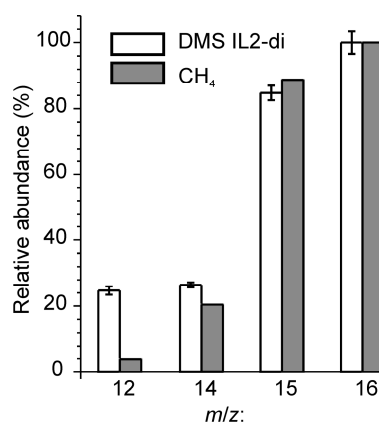


Figure 5. Relative intensities of signals from the group B and fragmentation patterns for electron impact ionization for CH_4 adapted from [59]. All the data were normalized by the signal m/z 16.

The excess of ions at m/z 12 and 14 can be related with the presence of butyl (C4) and propyl (C3) radicals among the emitted gas species. These radicals can be originated from homolytic cleavage of C–C or C–N bonds at butyl side chain attached to the cation. Previously it was suggested that part of C3 and C4 can reach a mass-spectrometer in a radical form due to their lower reactivity in comparison with methyl [44]. The stabilization increases with the increasing number of alkyl substituents on a radical centre because of hyperconjugation [63]. Due to the specifics of detachment from butyl side chains, C3 and C4 radicals should have one methyl and two or three methylene groups. Thus, the mass-spectrum of C3 and C4 radicals should have an excess of the ions at m/z 12-14 at the cost of the ions at m/z 15.

Correct attribution of the components of the group C to the ion fragments is not an easy task due to the large number of possible precursors, which can be emitted from the IL in molecular, radical or ionic forms. In the case of IL2 [44], the peaks m/z 24-48 were ascribed to a mixture of C2–C3 alkanes, their radicals and the products of non-oxidative decomposition of PEG including methyl and ethyl alcohols, noncyclic ethers, formaldehyde, acetic aldehyde, ethylene oxide, carbon mono- and dioxide among others [64]. The relative intensities of the components with m/z 24-34 determined in this study matched well the DMS of IL2 [44], but the DMS of IL2-di and IL2 differed in the range m/z 37-48. For IL2 the highest peak was at m/z 43, whereas for IL2-di it was at m/z 44. In comparison with IL2 the relative intensity of m/z 44 rose almost five-fold. This component can be ascribed to the ions $C_3H_8^+$, $C_2H_4O^+$ and CO_2^+ . The ion $C_3H_8^+$ is the principal ionized fragment of butane under electron ionization [59] and can originate from butyl side chain of the cation. For each cation IL2-di has twice butyl groups as IL2. In literature there is no information on the fragmentation patterns of alkyl and ethoxy radicals. However, it is reasonable to suggest that if butyl arrives at a mass-spectrometer as radical, the main ionized fragment could be the same as for butane, i.e. $C_3H_8^+$. This is because dissociation enthalpies of bonds adjacent to a radical centre decreases on 50-70 kcal/mole [63] and the dissociation under electron impact should be localized at the C–C· bond. A PEG monomer $-(CH_2)(CH_2)O\cdot$ can be detached from the polymer chain via tribochemical bond scission. This processes relies on the bond stretching that reduces the thermal energy required for cleavage of a bond [65,66]. In PEG, bond cleavage occurs mainly at C–O since the principal mass-spectral peaks of volatile products formed nonoxidative pyrolysis are CH_4O^+ and $C_2H_4O^+$ with m/z 32 and 44, respectively [67]. If the detached monomer is further non-dissociatively ionized the ion $C_2H_4O^+$ with m/z 44 can be formed. This differs from electron ionization of PEG, which yields $C_2H_5O^+$ with m/z 45 as the principal component. Finally, significant contribution from carbon dioxide is not expected since oxidative processes are hindered in vacuum.

The differences between IL2 and IL2-di imply that tribochemical stability of PEG chain decreased in dicationic configuration. This finding is in line with the results on thermal stability of dicationic ILs. Mahrova et al. [46] reported that thermal stability of dicationic *N*-alkylpyridinium ILs with PEG bridging chains decreased in comparison with an equivalent monocationic *N*-alkylpyridinium IL. Patil and coworkers [31] studied imidazolium, pyrrolidinium and phosphonium dicationic ILs with various lengths of alkane linkage chain and found that maximum thermal stability corresponded to C9 and decreased with further increasing of the linkage chain length. Emission of imidazolium head groups or its components could not be detected in this work in the range of m/z 1-120 that accords with the previous studies on tribochemical degradation [44,53], but contrasts with thermal [62] and X-ray radiation induced chemical degradation of *N*-alkylimidazolium cations [68]. Slightly lower chemical stability of IL2-di can favour passivation of metal surfaces and improve wear resistance.

For both IL2-di and IL2 the patterns of the NTf₂ anion tribochemical decomposition were alike. It can be related with the fact that the structure of the anion seems to be insensitive to the length of the linkage chain as well as to the number of the imidazolium head groups in the cation [30]. The results of the present study support the conclusions drawn in the previous work [44] that detachment of trifluoromethyl was the principal mechanism of the NTf₂ anion degradation on Ti substrates and contrast the findings of the work [27], in which NTf₂ tribochemical degradation on zirconia substrate was accompanied by emission of sulphates and/or sulphite. The difference in the

degradation steps of the anion on different substrates could be linked to the bond strength between the anion and the substrate. The anion can be immobilized on hydroxyl-terminated oxide surface by strong covalent bonding [27,33,69,70], while on partly oxidized metal surface only physical/chemical adsorption and hydrogen bonding occur. A covalently bonded anion can be subjected to larger strain under interfacial shearing and underwent more significant degradation, than an adsorbed anion. It is worth mentioning the similarity of the volatile products for the tribochemical degradation of the anion observed in the present work and X-ray radiation induced chemical degradation reported by Keppler et al. [68]. Both of these processes significantly differ from thermal degradation, which initiates from SO₂ release [62].

Deeper insight into the origin of various ions in the DMS as well as the tribochemical processes lying behind can be gained using behavioural analysis of the time series of the DMS signals [44]. Figure 6 shows several typical behaviours measured at two normal loads. In contrast with the IL2, the signals did not show well-defined behavioural patterns, rather complex behaviours, which can be characterized by superposition of various elemental patterns. At the lower load, two behavioural patterns were identified (Figure 6 (b) and (c)). The first one showed an intensive burst just at the beginning of the experiment followed by a transitional decay, which ceased even before the end of rubbing. The mass-spectral components with m/z 15, 51 and 69 (CH₃⁺, CHF₂⁺, CF₃⁺) among others behaved following this pattern. The second pattern was characterized by a step-wise increase at the beginning of rubbing and almost linear decreasing trend during rubbing. After the rubbing end the signal returned to the zero almost instantaneously. The mass-spectral peaks of group C mainly behaved following the second pattern. At the higher loads both patterns drastically changed. In the first pattern (Figure 6 (c)) after the initial burst the signals stabilized. After the rubbing end the signals transitionally returned to zero with a characteristic time constants in the range 150-250 s. In the second pattern (Figure 6 d) the decreasing trend switched to the growing one. After the rubbing end the signals slowly returned to zero with larger time constants, than in the first pattern.

In addition, a third pattern was identified for the mass-spectral peaks, which did not appeared at the lower load and corresponded to hydrogen and water (Figure 6 (a)). This pattern was characterized by a very slow dynamics and certain delays at the beginning of rubbing and at its end. This indicates that water and hydrogen emission was not directly related with tribochemical activation, rather with some secondary reactions. Our previous experiments have shown that the substrate and the pin could not be the sources of hydrogen or water. Neither had it to be the IL2-di since it was kept under vacuum for at least 48 hours before the experiment and water emission was not observed under the lower load.

Emission of H₂ and H₂O could be conceivably ascribed to the reactions of HF with Ti and TiO₂ [71]:



whereas HF can be formed as a product of the reaction of the anion with the hydroxyl-terminated surface of the alumina pin [70]. In fact, micro-Raman confocal and XPS analyses revealed the presence of TiF₃ and TiOF₂ on worn titanium surfaces lubricated with IL2 and other ILs with fluorinated anions [9,26,44].

Figure 7 shows the upper half of the correlation matrix of the DMS. The values of the Pearson correlation coefficients are codified by four grey levels. White cells correspond to those pairs of signals, for which the null hypothesis of the statistical significance of the correlation coefficient was not rejected. Strong correlation can be observed for m/z 2, 17 and 18 that supports the hypothesis of the common precursors and mechanisms of H₂ and H₂O emission. Also there is strong correlation within the following groups: (25, 26, 27), (27, 28, 29) and (30, 31). Moderate correlation can be observed between the peaks of the three groups: 14-16, 24-31 and 39-44, as well as between these peaks and m/z 51, 54 and 69. These findings suggest that the processes of anion and cation decomposition are much stronger correlated than for the monocationic IL2, for which the cationic and anionic decomposition products showed different emission behaviours.

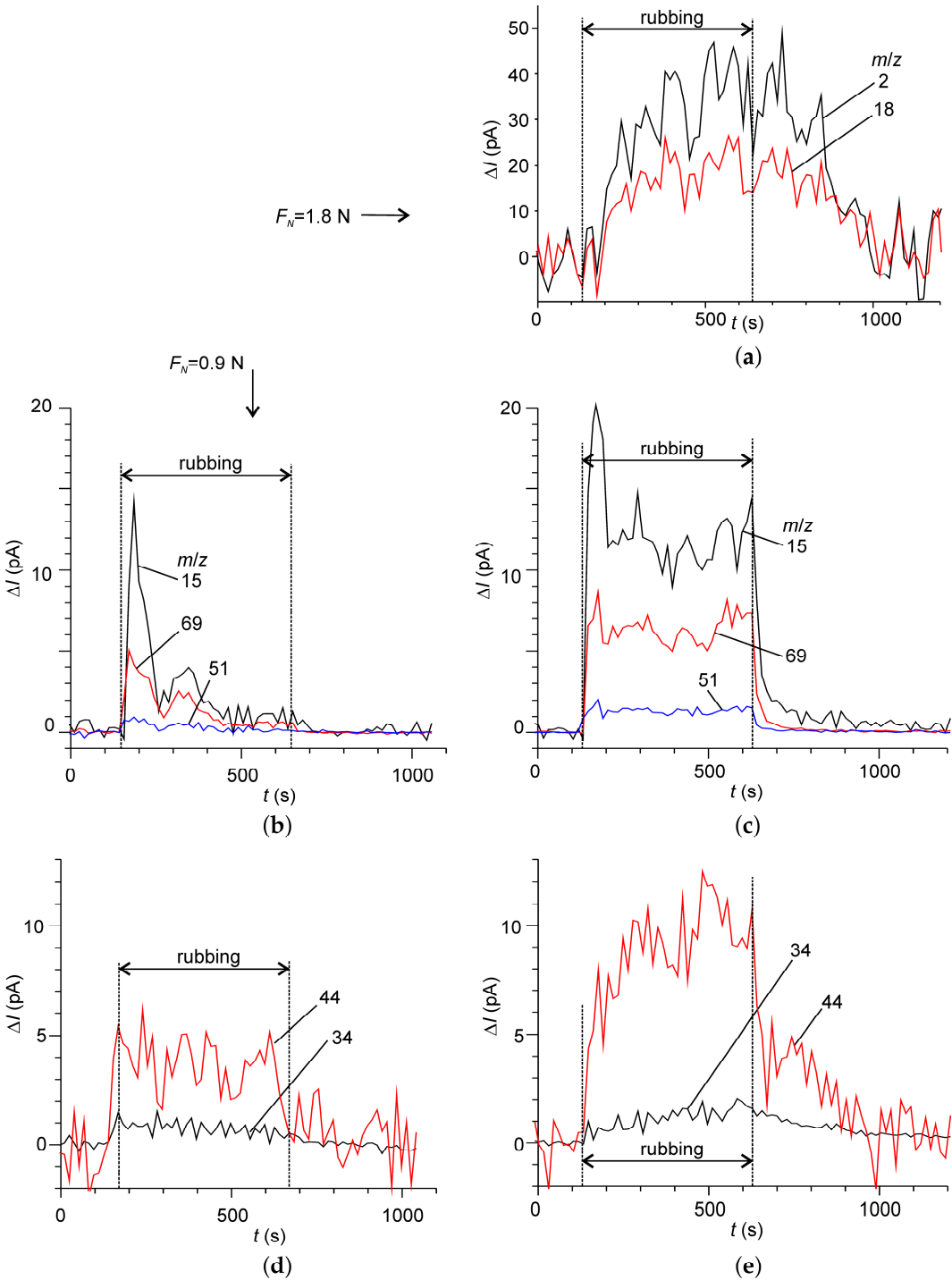


Figure 6. Some typical behaviour patterns of differential mass-spectrometric time series. (b) and (d) correspond to the load 0.9 N, whereas (a), (c) and (e) correspond to 1.8 N. The numbers at plot indicate the mass-to-charge ratio, m/z .

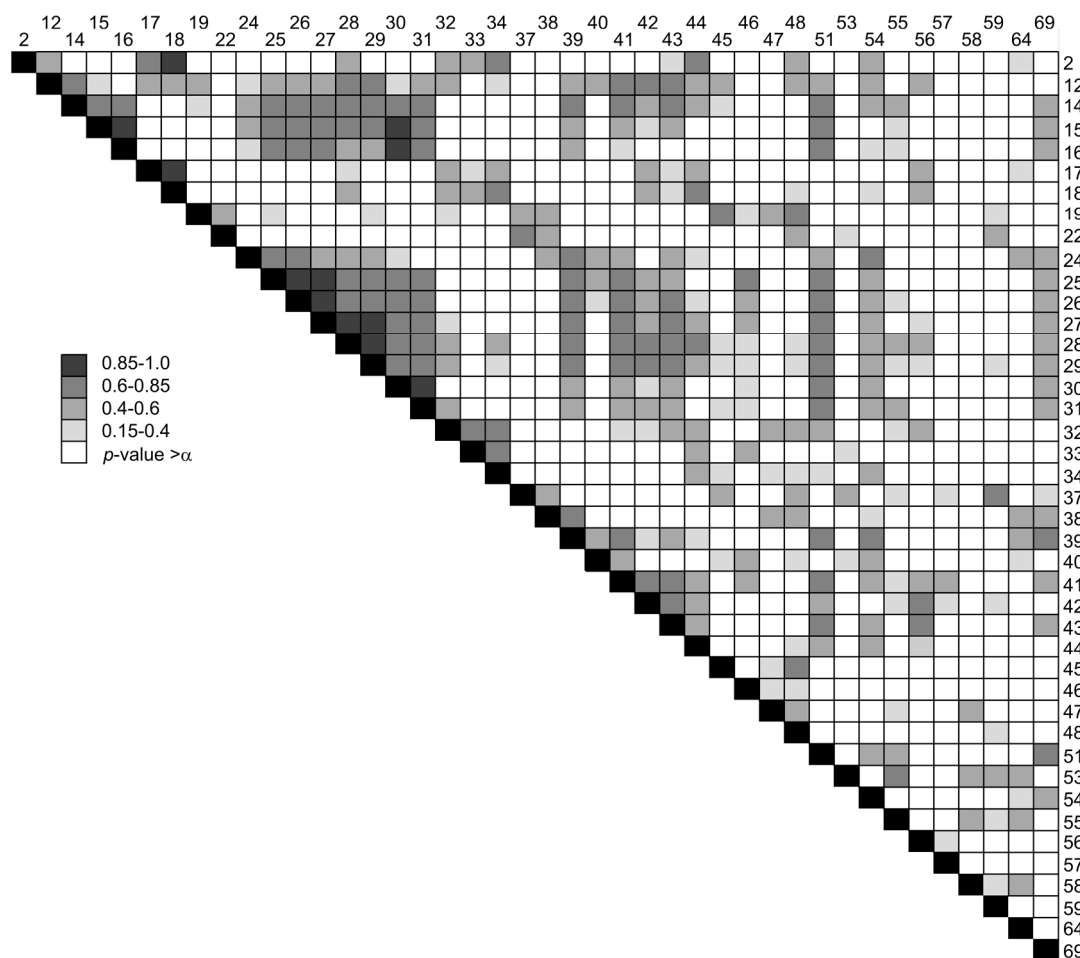


Figure 7. The upper half of the Pearson's correlation matrix for the DMS signals. The mass numbers of signals are shown at the rows and columns. The colour scale indicates the values of Pearson's coefficient of correlation.

The observed changes in triboemission behaviour with the normal load could be interpreted in terms of formation and wearing off the protective tribofilm. Under given mild experimental conditions frictional heating should be discarded as a driving force of tribochemical reactions [72-74]. It should be noted that under low sliding velocity, like in this study, the molecules in the liquid phase could not be strained sufficiently to trigger tribochemical reactions. Only the molecules bonded to the surface could be subjected to sufficient strain. So, the volatiles detected in this study had to originate from the tribofilm. Although a tribofilm was not analysed in this study, there is plenty of experimental evidences that dicationic ILs with longer bridging chain tended to adsorb on the surface creating large aggregate structures and exhibiting better packing than monocationic ILs [29,75]. Better lubricity of the IL2-di in comparison with the IL2 can be associated to these compact aggregate structures and higher surface activity of dicationic ILs with larger spacer lengths [75]. Under the lower normal load compact aggregate structures could probably accommodate the interfacial shear and protect the substrate from damage. Weak bonding between the ions in the aggregate layer prevented the anions from stretching and intensive tribochemical decomposition. Thus, after short run in the emission of the decomposition products corresponding to the anion completely ceased. On the other hand, the emission of fragments of the side and bridging chains of the cationic moiety could be related with distinguishing features of the molecular structure of the dicationic ILs. For longer bridging chains, e.g. larger than 6 methylene groups, two imidazolium rings tended to position themselves above and below each other forming π - π stacking interactions, and the bridge chain extended perpendicularly to the imidazolium ring [38]. In this work we carried out simple molecular mechanics modelling using Chem3D Pro in order to determine optimal 3-dimensional arrangement of atoms in the cation representing a local energy minimum. The results

are shown in Figure 8. Although only a single cation was modelled and the electrons were not explicitly considered in the modelling, in the majority of stable molecular conformation found by the modelling the cation tended to fold over the PEG bridging chain with two imidazolium heads approaching each other.

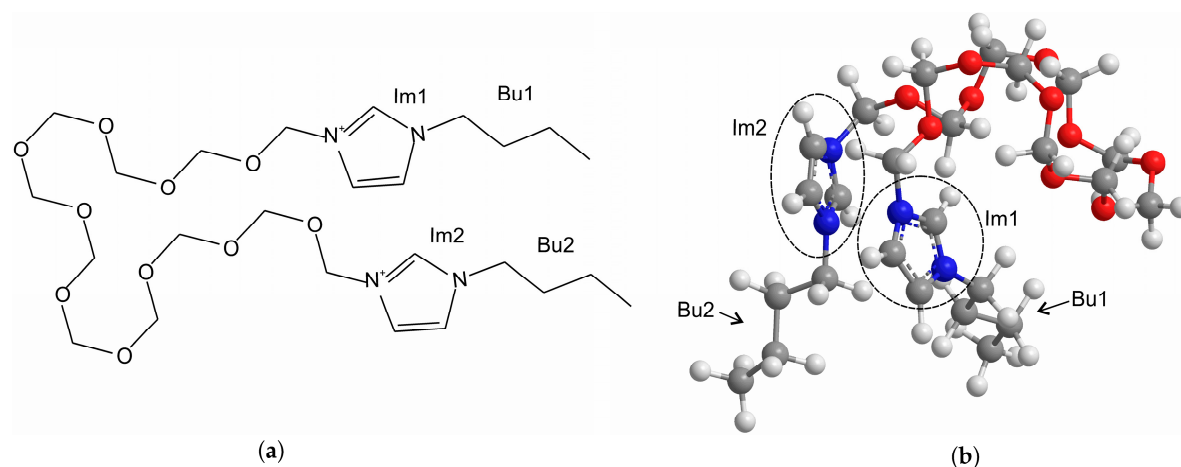


Figure 8. Optimized 3-dimensional stable molecular conformation of the cation of dicationic IL representing a local energy minimum. a) 2-dimensional structure; b) 3-dimensional structure. Im1 and Im2 are the imidazolium head groups; Bu1 and Bu2 are the butyl side chains. The atoms are represented by the following colours: H - white, C - grey, N - blue and O - red.

Some chain-chain interaction was reported for alkyl chains with 12 or more methylene groups [30]. The conformation of the cation having the imidazolium heads bonded to each other and to a substrate and the side and the bridging chains protruding outside can probably be a reason for continuous emission of cationic fragments even under low load. With the increasing normal load both the cation and anion degradation intensified. On the other hand, removal of the aggregate adsorbed layer under the higher load could allow HF to attack the surface. Slow dynamics of water and hydrogen emission could be related with slow diffusion through the IL followed by desorption from its surface.

4. Conclusions

Mechanically stimulated gas emission spectrometry was applied for studying dynamic triboemission processes in germinal dicationic IL with *N*-alkylimidazolium cation head groups, PEG bridging chain and bis(trifluoromethanesulfonyl)imide anion. Homologous monocationic IL was taken as a benchmark. It was found that dicationic IL had better lubricity. Friction coefficient was stable without noticeable run in. The general structures of the mass-spectra of volatile components emitted from the dicationic and monocationic ILs were alike. However, the dicationic IL had much stronger peak at m/z 44, which was ascribed to a monomer of PEG and butyl. This implies less tribochemical stability of PEG as a bridging chain, than a free side chain. Tribochemical decomposition of the anion seemed insensitive to the number of the cationic head groups. The behaviour of mass-spectral time series significantly varied with the applied normal load. At the lower load the signals tended to decrease during rubbing, while at the higher load they increased. In contrast with the homologous monocationic IL the time series of the ions originated from cation precursors and anion precursors showed good correlation. The complex behaviour of the mechanically stimulated gas emission was interpreted in terms of dynamic formation and destruction of a protective tribofilm. Mechanically stimulated gas emission mass-spectrometry has been proven as a powerful tool for dynamic analysis of complex tribochemical processes.

Acknowledgments: The authors are grateful to M. Mahrova for providing the synthesized IL. The authors acknowledge the help of O. Sanchez in measuring the surface profiles. This work was supported by the Ministry of Economy and Competitiveness of Spain through the grant BIA2016-79528-R.

Author Contributions: R.N. and M.C. conceived, designed and performed the experiments; S.G. participated in performing the experiments and data treatment; R.N. and S.G. analyzed the data; E.R. contributed to the analysis and interpretation of the data; R.N. wrote the paper.

Conflicts of Interest: The authors declare no conflict of interest.

References

- Bermúdez, M.-D.; Jiménez, A.-E.; Sanes, J.; Carrión, F.-J. Ionic liquids as advanced lubricant fluids. *Molecules* 2009, 14, 2888-2908.
- Somers, A.; Howlett, P.; MacFarlane, D.; Forsyth, M. A review of ionic liquid lubricants. *Lubricants* 2013, 1, 3-21.
- Mordukhovich, G.; Qu, J.; Howe, J.Y.; Bair, S.; Yu, B.; Luo, H.; Smolenski, D.J.; Blau, P.J.; Bunting, B.G.; Dai, S. A low-viscosity ionic liquid demonstrating superior lubricating performance from mixed to boundary lubrication. *Wear* 2013, 301, 740-746.
- Gutierrez, M.; Haselkorn, M.; Iglesias, P. The lubrication ability of ionic liquids as additives for wind turbine gearboxes oils. *Lubricants* 2016, 4, 14.
- Yu, B.; Bansal, D.G.; Qu, J.; Sun, X.; Luo, H.; Dai, S.; Blau, P.J.; Bunting, B.G.; Mordukhovich, G.; Smolenski, D.J. Oil-miscible and non-corrosive phosphonium-based ionic liquids as candidate lubricant additives. *Wear* 2012, 289, 58-64.
- Somers, A.; Yunis, R.; Armand, M.; Pringle, J.; MacFarlane, D.; Forsyth, M. Towards phosphorus free ionic liquid anti-wear lubricant additives. *Lubricants* 2016, 4, 22.
- Huang, G.; Yu, Q.; Ma, Z.; Cai, M.; Liu, W. Probing the lubricating mechanism of oil-soluble ionic liquids additives. *Tribology International* 2017, 107, 152-162.
- Cai, M.; Liang, Y.; Yao, M.; Xia, Y.; Zhou, F.; Liu, W. Imidazolium ionic liquids as antiwear and antioxidant additive in poly(ethylene glycol) for steel/steel contacts. *ACS Applied Materials & Interfaces* 2010, 2, 870-876.
- Gabler, C.; Dörr, N.; Allmaier, G. Influence of cationic moieties on the tribolayer constitution shown for bis(trifluoromethylsulfonyl)imide based ionic liquids studied by X-ray photoelectron spectroscopy. *Tribology International* 2014, 80, 90-97.
- Pisarova, L.; Gabler, C.; Dörr, N.; Pittenauer, E.; Allmaier, G. Thermo-oxidative stability and corrosion properties of ammonium based ionic liquids. *Tribology International* 2012, 46, 73-83.
- Minami, I. Ionic liquids in tribology. *Molecules* 2009, 14, 2286-2305.
- Morales, W.; Street, K.W.J.; Rychard, R.M.; Valco, D. Tribological testing and thermal analysis of an alkyl sulfate series of ionic liquids for use as aerospace lubricants. *Tribology Transactions* 2012, 55, 815-821.
- Zhang, S.; Hu, L.; Qiao, D.; Feng, D.; Wang, H. Vacuum tribological performance of phosphonium-based ionic liquids as lubricants and lubricant additives of multialkylated cyclopentanes. *Tribology International* 2013, 66, 289-295.
- Jin, C.-M.; Ye, C.; Phillips, B.S.; Zabinski, J.S.; Liu, X.; Liu, W.; Shreeve, J.n.M. Polyethylene glycol functionalized dicationic ionic liquids with alkyl or polyfluoroalkyl substituents as high temperature lubricants. *Journal of Materials Chemistry* 2006, 16, 1529-1535.
- Jiménez, A.; Bermúdez, M.-D. Ionic liquids as lubricants of titanium–steel contact. *Tribology Letters* 2009, 33, 111-126.
- Jiménez, A.E.; Bermúdez, M.D.; Iglesias, P.; Carrión, F.J.; Martínez-Nicolás, G. 1-n-alkyl-3-methylimidazolium ionic liquids as neat lubricants and lubricant additives in steel–aluminium contacts. *Wear* 2006, 260, 766-782.
- Jiménez, A.-E.; Bermúdez, M.-D. Imidazolium ionic liquids as additives of the synthetic ester propylene glycol dioleate in aluminium–steel lubrication. *Wear* 2008, 265, 787-798.
- Barnhill, W.C.; Qu, J.; Luo, H.; Meyer, H.M.; Ma, C.; Chi, M.; Papke, B.L. Phosphonium-organophosphate ionic liquids as lubricant additives: Effects of cation structure on physicochemical and tribological characteristics. *ACS Applied Materials & Interfaces* 2014, 6, 22585-22593.
- Pejaković, V.; Tomastik, C.; Dörr, N.; Kalin, M. Influence of concentration and anion alkyl chain length on tribological properties of imidazolium sulfate ionic liquids as additives to glycerol in steel–steel contact lubrication. *Tribology International* 2016, 97, 234-243.

20. Mu, Z.; Zhou, F.; Zhang, S.; Liang, Y.; Liu, W. Effect of the functional groups in ionic liquid molecules on the friction and wear behavior of aluminum alloy in lubricated aluminum-on-steel contact. *Tribology International* 2005, 38, 725-731.
21. Cai, M.; Zhao, Z.; Liang, Y.; Zhou, F.; Liu, W. Alkyl imidazolium ionic liquids as friction reduction and anti-wear additive in polyurea grease for steel/steel contacts. *Tribology Letters* 2010, 40, 215-224.
22. Xiao, H.; Guo, D.; Liu, S.; Pan, G.; Lu, X. Film thickness of ionic liquids under high contact pressures as a function of alkyl chain length. *Tribology Letters* 2011, 41, 471-477.
23. Fan, M.; Song, Z.; Liang, Y.; Zhou, F.; Liu, W. Laxative inspired ionic liquid lubricants with good detergency and no corrosion. *ACS Applied Materials & Interfaces* 2014, 6, 3233-3241.
24. Ye, C.; Liu, W.; Chen, Y.; Yu, L. Room-temperature ionic liquids: A novel versatile lubricant. *Chemical Communications* 2001, 2244-2245.
25. Zhou, F.; Liang, Y.; Liu, W. Ionic liquid lubricants: Designed chemistry for engineering applications. *Chemical Society Reviews* 2009, 38, 2590-2599.
26. Jiménez, A.E.; Bermúdez, M.D. Ionic liquids as lubricants of titanium-steel contact. Part 3. Ti6Al4V lubricated with imidazolium ionic liquids with different alkyl chain lengths. *Tribology Letters* 2010, 40, 237-246.
27. Mahrova, M.; Conte, M.; Roman, E.; Nevshupa, R. Critical insight into mechanochemical and thermal degradation of imidazolium-based ionic liquids with alkyl and monomethoxypoly(ethylene glycol) side chains. *Journal of Physical Chemistry C* 2014, 118, 22544-22552.
28. Li, S.; Feng, G.; Bañuelos, J.L.; Rother, G.; Fulvio, P.F.; Dai, S.; Cummings, P.T. Distinctive nanoscale organization of dicationic versus monocationic ionic liquids. *The Journal of Physical Chemistry C* 2013, 117, 18251-18257.
29. Shirota, H.; Ishida, T. Microscopic aspects in dicationic ionic liquids through the low-frequency spectra by femtosecond Raman-induced KERR effect spectroscopy. *The Journal of Physical Chemistry B* 2011, 115, 10860-10870.
30. Bodo, E.; Chiricotto, M.; Caminiti, R. Structure of geminal imidazolium bis(trifluoromethylsulfonyl)imide dicationic ionic liquids: A theoretical study of the liquid phase. *The Journal of Physical Chemistry B* 2011, 115, 14341-14347.
31. Patil, R.A.; Talebi, M.; Xu, C.; Bhawal, S.S.; Armstrong, D.W. Synthesis of thermally stable geminal dicationic ionic liquids and related ionic compounds: An examination of physicochemical properties by structural modification. *Chemistry of Materials* 2016, 28, 4315-4323.
32. Pagano, F.; Gabler, C.; Zare, P.; Mahrova, M.; Dörr, N.; Bayon, R.; Fernandez, X.; Binder, W.; Hernaiz, M.; Tojo, E., et al. Dicationic ionic liquids as lubricants. *Proceedings of the Institution of Mechanical Engineers, Part J: Journal of Engineering Tribology* 2012, 226, 952-964.
33. Palacio, M.; Bhushan, B. Molecularly thick dicationic ionic liquid films for nanolubrication. *Journal of Vacuum Science & Technology A* 2009, 27, 986-995.
34. Czerniak, K.; Walkiewicz, F. Synthesis and antioxidant properties of dicationic ionic liquids. *New Journal of Chemistry* 2017, 41, 530-539.
35. Chang, J.-C.; Ho, W.-Y.; Sun, I.W.; Tung, Y.-L.; Tsui, M.-C.; Wu, T.-Y.; Liang, S.-S. Synthesis and characterization of dicationic ionic liquids that contain both hydrophilic and hydrophobic anions. *Tetrahedron* 2010, 66, 6150-6155.
36. Gindri, I.M.; Siddiqui, D.A.; Frizzo, C.P.; Martins, M.A.P.; Rodrigues, D.C. Improvement of tribological and anti-corrosive performance of titanium surfaces coated with dicationic imidazolium-based ionic liquids. *RSC Advances* 2016, 6, 78795-78802.
37. Khan, A.S.; Man, Z.; Arvina, A.; Bustam, M.A.; Nasrullah, A.; Ullah, Z.; Sarwono, A.; Muhammad, N. Dicationic imidazolium based ionic liquids: Synthesis and properties. *Journal of Molecular Liquids* 2017, 227, 98-105.
38. Serva, A.; Migliorati, V.; Lapi, A.; Aquilanti, G.; Arcovito, A.; D'Angelo, P. Structural properties of geminal dicationic ionic liquid/water mixtures: A theoretical and experimental insight. *Physical Chemistry Chemical Physics* 2016, 18, 16544-16554.
39. Anderson, J.L.; Ding, R.; Ellern, A.; Armstrong, D.W. Structure and properties of high stability geminal dicationic ionic liquids. *Journal of the American Chemical Society* 2005, 127, 593-604.

40. Shirota, H.; Mandai, T.; Fukazawa, H.; Kato, T. Comparison between dicationic and monocationic ionic liquids: Liquid density, thermal properties, surface tension, and shear viscosity. *Journal of Chemical & Engineering Data* 2011, 56, 2453-2459.
41. Zeng, Z.; Phillips, B.S.; Xiao, J.-C.; Shreeve, J.n.M. Polyfluoroalkyl, polyethylene glycol, 1,4-bismethylenebenzene, or 1,4-bismethylene-2,3,5,6-tetrafluorobenzene bridged functionalized dicationic ionic liquids: Synthesis and properties as high temperature lubricants. *Chemistry of Materials* 2008, 20, 2719-2726.
42. Minami, I.; Inada, T.; Sasaki, R.; Nanao, H. Tribo-chemistry of phosphonium-derived ionic liquids. *Tribology Letters* 2010, 40, 225-235.
43. Jiménez, A.E.; Bermúdez, M.D. Short alkyl chain imidazolium ionic liquid additives in lubrication of three aluminium alloys with synthetic ester oil. *Tribology - Materials, Surfaces & Interfaces* 2012, 6, 109-115.
44. Nevshupa, R.; Conte, M.; del Campo, A.; Roman, E. Analysis of tribochemical decomposition of two imidazolium ionic liquids on Ti-6Al-4V through mechanically stimulated gas emission spectrometry. *Tribology International* 2016, 102, 19-27.
45. Cai, M.; Liang, Y.; Zhou, F.; Liu, W. A novel imidazolium salt with antioxidation and anticorrosion dual functionalities as the additive in poly(ethylene glycol) for steel/steel contacts. *Wear* 2013, 306, 197-208.
46. Mahrova, M.; Pagano, F.; Pejakovic, V.; Valea, A.; Kalin, M.; Igartua, A.; Tojo, E. Pyridinium based dicationic ionic liquids as base lubricants or lubricant additives. *Tribology International* 2015, 82, Part A, 245-254.
47. Bermúdez, M.-D.; Jiménez, A.-E.; Sanes, J.; Carrión, F.-J. Ionic liquids as advanced lubricant fluids. *Molecules* 2009, 14, 2888.
48. Lu, R.; Mori, S.; Kobayashi, K.; Nanao, H. Study of tribochemical decomposition of ionic liquids on a nascent steel surface. *Applied Surface Science* 2009, 255, 8965-8971.
49. Nevchoupa, R.A.; De Segovia, J.L.; Deulin, E.A. An uhv system to study gassing and outgassing of metals under friction. *Vacuum* 1999, 52, 73-81.
50. Nevshupa, R.A.; Conte, M.; Igartua, A.; Roman, E.; de Segovia, J.L. Ultrahigh vacuum system for advanced tribology studies: Design principles and applications. *Tribology International* 2015, 86, 28-35.
51. Okubo, H.; Sasaki, S. In situ raman observation of structural transformation of diamond-like carbon films lubricated with modtc solution: Mechanism of wear acceleration of DLC films lubricated with modtc solution. *Tribology International* 2017, 113, 399-410.
52. Merkle, A.P.; Erdemir, A.; Eryilmaz, O.L.; Johnson, J.A.; Marks, L.D. In situ TEM studies of tribo-induced bonding modifications in near-frictionless carbon films. *Carbon* 2010, 48, 587-591.
53. Kawada, S.; Watanabe, S.; Kondo, Y.; Tsuboi, R.; Sasaki, S. Tribochemical reactions of ionic liquids under vacuum conditions. *Tribology Letters* 2014, 54, 309-315.
54. Nevshupa, R.; Grinkevich, K.E.; Martinez, I.; Roman, E. Trides – a new tool for the design, development and non-destructive evaluation of advanced construction steels. *Materiales de Construcción* 2016, 66, e099.
55. Zare, P.; Mahrova, M.; Tojo, E.; Stojanovic, A.; Binder, W.H. Ethylene glycol-based ionic liquids via azide/alkyne click chemistry. *Journal of Polymer Science Part A: Polymer Chemistry* 2013, 51, 190-202.
56. Nevshupa, R.A.; Roman, E.; de Segovia, J.L. Origin of hydrogen desorption during friction of stainless steel by alumina in ultrahigh vacuum. *Journal of Vacuum Science & Technology A* 2008, 26, 1218-1223.
57. Rusanov, A.; Nevshupa, R.; Fontaine, J.; Martin, J.-M.; Le Mogne, T.; Elinson, V.; Lyamin, A.; Roman, E. Probing the tribochemical degradation of hydrogenated amorphous carbon using mechanically stimulated gas emission spectroscopy. *Carbon* 2015, 81, 788-799.
58. Roman, E.; Conte, M.; Nevshupa, R. In Time-resolved tribochemistry of ionic liquids, *Lubmat: Lubrication, Maintenance and Tribology Bilbao*, June 7-8, 2016, 2016; Aranzabe, A., Ed. IK4-Tekniker: Bilbao.
59. Stein (director), S.E. "Mass spectra" by nist mass spec data center. In NIST chemistry webbook, NIST standard reference database number 69, Linstrom, P.J.; Mallard, W.G., Eds. National Institute of Standards and Technology: Gaithersburg MD, 2017.
60. Rusanov, A.; Nevshupa, R.; Martin, J.-M.; Garrido, M.Á.; Roman, E. Tribochemistry of hydrogenated amorphous carbon through analysis of mechanically stimulated gas emission. *Diamond and Related Materials* 2015, 55, 32-40.

61. Köddermann, T.; Wertz, C.; Heintz, A.; Ludwig, R. Ion-pair formation in the ionic liquid 1-ethyl-3-methylimidazolium bis(triflyl)imide as a function of temperature and concentration. *ChemPhysChem* 2006, 7, 1944-1949.
62. Kroon, M.C.; Buijs, W.; Peters, C.J.; Witkamp, G.-J. Quantum chemical aided prediction of the thermal decomposition mechanisms and temperatures of ionic liquids. *Thermochimica Acta* 2007, 465, 40-47.
63. Zhang, X.-M. Homolytic bond dissociation enthalpies of the c-h bonds adjacent to radical centers. *The Journal of Organic Chemistry* 1998, 63, 1872-1877.
64. Pielichowski, K.; Flejtuch, K. Non-oxidative thermal degradation of poly(ethylene oxide): Kinetic and thermoanalytical study. *Journal of Analytical and Applied Pyrolysis* 2005, 73, 131-138.
65. Boldyrev, V.V. Mechanochemistry and mechanical activation of solids. *Russian Chemical Reviews* 2006, 75, 177-190.
66. Ribas-Arino, J.; Marx, D. Covalent mechanochemistry: Theoretical concepts and computational tools with applications to molecular nanomechanics. *Chemical Reviews* 2012, 112, 5412-5487.
67. Kitahara, Y.; Takahashi, S.; Fujii, T. Thermal analysis of polyethylene glycol: Evolved gas analysis with ion attachment mass spectrometry. *Chemosphere* 2012, 88, 663-669.
68. Keppler, A.; Himmerlich, M.; Ikari, T.; Marschewski, M.; Pachomow, E.; Hoff, O.; Maus-Friedrichs, W.; Endres, F.; Krischok, S. Changes of the near-surface chemical composition of the 1-ethyl-3-methylimidazolium bis(trifluoromethylsulfonyl)imide room temperature ionic liquid under the influence of irradiation. *Physical Chemistry Chemical Physics* 2011, 13, 1174-1181.
69. Nainaparampil, J.J.; Phillips, B.S.; Eapen, K.C.; Zabinski, J.S. Micro-nano behaviour of dmbi-pf 6 ionic liquid nanocrystals: Large and small-scale interfaces. *Nanotechnology* 2005, 16, 2474.
70. Valkenberg, M.H.; deCastro, C.; Holderich, W.F. Immobilisation of ionic liquids on solid supports. *Green Chemistry* 2002, 4, 88-93.
71. Buslaev, Y.A.; Bochkareva, V.A.; Nikolaev, N.S. The reaction of titanium dioxide with hydrofluoric acid. *Bulletin of the Academy of Sciences of the USSR, Division of chemical science* 1962, 11, 361-364.
72. Walton, A.J. Triboluminescence. *Advances in Physics* 1977, 26, 887-948.
73. Nevshupa, R. The role of athermal mechanisms in the activation of tribodesorption and triboluminescence in miniature and lightly loaded friction units. *Journal of Friction and Wear* 2009, 30, 118-126.
74. Nevshupa, R.A.; Roman, E.; de Segovia, J.L. Model of the effect of local frictional heating on the tribodesorbed gases from metals in ultra-high vacuum. *International Journal of Materials and Product Technology* 2010, 38, 57-65.
75. Frizzo, C.P.; Gindri, I.M.; Bender, C.R.; Tier, A.Z.; Villetti, M.A.; Rodrigues, D.C.; Machado, G.; Martins, M.A.P. Effect on aggregation behavior of long-chain spacers of dicationic imidazolium-based ionic liquids in aqueous solution. *Colloids and Surfaces A: Physicochemical and Engineering Aspects* 2015, 468, 285-294.